

(19) World Intellectual Property Organization
International Bureau



(43) International Publication Date
21 February 2008 (21.02.2008)

PCT

(10) International Publication Number
WO 2008/021358 A2

(51) International Patent Classification:
C21D 1/00 (2006.01) C22C 45/00 (2006.01)

(74) Agent: GREEN, Robert, A.; Christie, Parker & Hale, LLP, P.O. box 7068, Pasadena, CA 91109-7068 (US).

(21) International Application Number:
PCT/US2007/017983

(81) Designated States (unless otherwise indicated, for every kind of national protection available): AE, AG, AL, AM, AT, AU, AZ, BA, BB, BG, BH, BR, BW, BY, BZ, CA, CH, CN, CO, CR, CU, CZ, DE, DK, DM, DO, DZ, EC, EE, EG, ES, FI, GB, GD, GE, GH, GM, GT, HN, HR, HU, ID, IL, IN, IS, JP, KE, KG, KM, KN, KP, KR, KZ, LA, LC, LK, LR, LS, LT, LU, LY, MA, MD, ME, MG, MK, MN, MW, MX, MY, MZ, NA, NG, NI, NO, NZ, OM, PG, PH, PL, PT, RO, RS, RU, SC, SD, SE, SG, SK, SL, SM, SV, SY, TJ, TM, TN, TR, TT, TZ, UA, UG, US, UZ, VC, VN, ZA, ZM, ZW.

(22) International Filing Date: 13 August 2007 (13.08.2007)

(25) Filing Language: English

(26) Publication Language: English

(30) Priority Data:
60/837,176 11 August 2006 (11.08.2006) US

(71) Applicant (for all designated States except US): CALIFORNIA INSTITUTE OF TECHNOLOGY [US/US]; 1200 East California Boulevard, Mail Stop 201-85, Pasadena, CA 91125 (US).

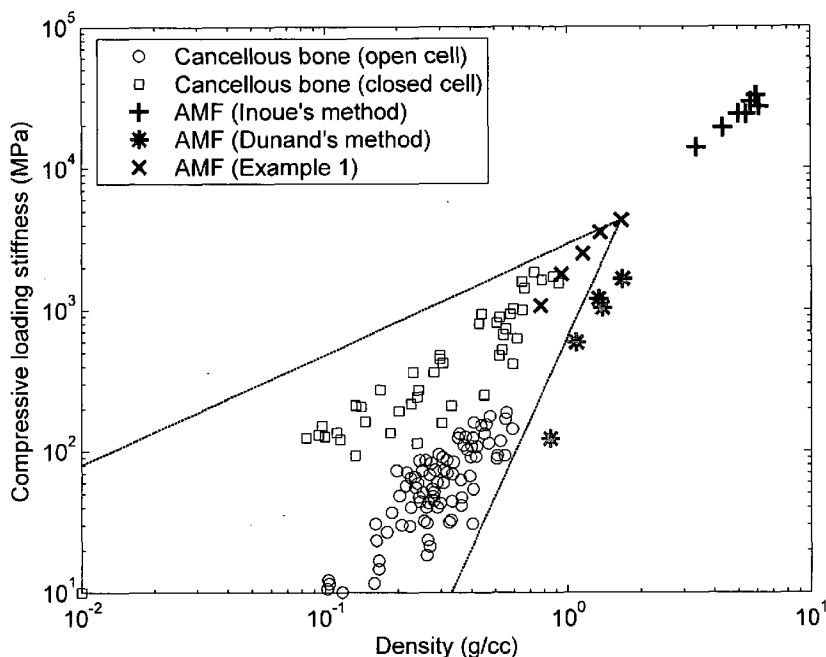
(84) Designated States (unless otherwise indicated, for every kind of regional protection available): ARIPO (BW, GH, GM, KE, LS, MW, MZ, NA, SD, SL, SZ, TZ, UG, ZM, ZW), Eurasian (AM, AZ, BY, KG, KZ, MD, RU, TJ, TM), European (AT, BE, BG, CH, CY, CZ, DE, DK, EE, ES, FI, FR, GB, GR, HU, IE, IS, IT, LT, LU, LV, MC, MT, NL, PL, PT, RO, SE, SI, SK, TR), OAPI (BF, BJ, CF, CG, CI, CM, GA, GN, GQ, GW, ML, MR, NE, SN, TD, TG).

(72) Inventors; and

(75) Inventors/Applicants (for US only): DEMETRIOU, Marios, D. [US/US]; 120 South Swall Drive, Apt. 105, Los Angeles, CA 90048 (US). HARMON, John, S. [US/US]; 30 North Greenwood Avenue, Pasadena, CA 91107 (US). JOHNSON, William, L. [US/US]; 3546 Mountain View Avenue, Pasadena, CA 91107 (US). VEAZEY, Chris [US/US]; 94 South Parkwood, Unit D, Pasadena, CA 91107 (US).

Published:
— without international search report and to be republished upon receipt of that report

(54) Title: AMORPHOUS METAL FOAM AS A PROPERTY-MATCHED BONE SCAFFOLD SUBSTITUTE



(57) Abstract: Amorphous metal foams and methods of making the same are provided. The amorphous metal foams have properties matching those of natural bone, enabling their use as bone replacement scaffolds. In one embodiment, for example, an amorphous metal foam has a density-dependent stiffness (or Young's modulus, denoted E) ranging from about $640p^{3.75}$ to above $2900p^{0.78}$, and a density dependent strength (p_y) greater than about $8.1p^{2.57}$, wherein p (the density) is less than about 1.7 g/cc.

WO 2008/021358 A2

1 **AMORPHOUS METAL FOAM AS A PROPERTY-MATCHED**
 BONE SCAFFOLD SUBSTITUTE

FIELD OF THE INVENTION

5 **[0001]** The invention is directed to amorphous metal foams having properties matching those of bone, enabling their use as bone replacements.

BACKGROUND OF THE INVENTION

10 **[0002]** Porous metallic scaffold substitutes for the replacement of damaged natural bone have been steadily gaining interest. Indeed, porous titanium and tantalum scaffold materials exhibiting good biocompatibility and bioactivity are currently commercially available. Nevertheless, from a mechanical perspective, these scaffolds are still considered inadequate for replicating the unique mechanical performance of natural bone, which is characterized by high strength, high specific strength, and low stiffness. This mechanical inadequacy is
15 primarily attributed to the relatively low strength and high modulus of pure crystalline metals, which characteristics are inherited by the porous counterparts, resulting in poor replication of the load bearing capabilities of bone.

20 **[0003]** Another drawback of conventional porous metals is their inability to be processed into near-net-shapes, which is attributed to the poor superplasticity that characterizes conventional crystalline metals. Owing to this inability, the complexity of free-form fabrication of porous metallic scaffolds increases dramatically, resulting in substantially high manufacturing costs.

SUMMARY OF THE INVENTION

25 **[0004]** The invention is directed to amorphous metal foams (AMFs) having density-dependent stiffnesses and density-dependent strengths closely matching those of natural bone. Compared to crystalline metals, amorphous metals exhibit considerably higher strengths and notably lower moduli, suggesting a mechanical performance for their porous counterparts capable of closely replicating the load bearing capabilities of bone. More
30 interestingly, the ability of amorphous metals to be "net-shaped" thermoplastically when softened gives rise to a potentially efficient scaffold fabrication technology.

35 **[0005]** In one embodiment, AMFs exhibit both density-dependent strengths and stiffnesses that fall inside the respective ranges for bone. For example, in one embodiment, an AMF exhibits a density-dependent stiffness that substantially matches that of bone, and exhibits a density-dependent strength that is substantially equal to or greater than that of bone. In one exemplary embodiment, the AMF exhibits a density-dependent stiffness ranging from about $E = 640\rho^{3.75}$ to about $E = 2900\rho^{0.78}$, where $\rho < 1.7$ g/cc, and a density-dependent strength greater than about $\sigma_y = 8.1\rho^{2.57}$, where $\rho < 1.7$ g/cc.

1 [0006] The AMFs according to the present invention may be synthesized by any suitable
method so long as the resulting AMF has the desired stiffness and strength properties.
According to one exemplary embodiment, an AMF is produced by first producing a two-
phase mixture of a suitable alloy in its liquid state and a chemically non-reacting propellant
5 gas. The mixture is placed in an inert gas atmosphere under a pressure, p_i . The mixture is
held a temperature T_i that is greater than the optimum temperature for foaming, T_o . The
mixture is then brought to the optimum temperature T_o , and foam expansion is induced by
dropping the pressure to the optimum pressure, p_o , where $p_o < p_i$. The two-phase mixture is
then quenched to a temperature below the glass transition temperature of the alloy, thereby
10 producing an amorphous metal foam.

BRIEF DESCRIPTION OF THE DRAWINGS

[0007] The patent or application file contains at least one drawing executed in color.
Copies of this patent or patent application publication with color drawing(s) will be provided
15 by the office upon request and payment of the necessary fee.

[0008] The above and other features and advantages of the present invention will be
better understood with reference to the following detailed description when considered in
conjunction with the attached drawings in which:

- [0009] FIG. 1A is a time-temperature-transformation diagram of $\text{Pd}_{43}\text{Ni}_{10}\text{Cu}_{27}\text{P}_{20}$ liquid;
20 [0010] FIG. 1B is a plot of the temperature-dependent viscosity of $\text{Pd}_{43}\text{Ni}_{10}\text{Cu}_{27}\text{P}_{20}$
liquid;
[0011] FIG. 1C is a plot of the limits of strain rate sensitivity of $\text{Pd}_{43}\text{Ni}_{10}\text{Cu}_{27}\text{P}_{20}$ liquid;
[0012] FIG. 2 is a photograph of an amorphous metal foam (AMF) produced according to
Example 1 and having a density of 1.16 g/cc (88% porosity);
25 [0013] FIG 3 is an X-ray diffractogram verifying the amorphous nature of the AMF
produced according to Example 1 having a density of 1.16 g/cc;
[0014] FIG. 4 is a photograph of two AMFs prepared according to Example 1 floating in
water, each AMF having a density of 0.93 g/cc (90% porosity);
[0015] FIG. 5 is a graph comparing the compressive loading response of an amorphous
30 metal foam prepared according to Example 1 to the compressive loading response of
trabecular (or cancellous) bone;
[0016] FIG. 6 is a graph comparing the compressive strength vs. Young's Modulus plot of
an amorphous metal foam prepared according to Example 1 to the compressive strength vs.
Young's Modulus plot of trabecular (or cancellous) bone;
35 [0017] FIG. 7A is a graph comparing the specific stiffness vs. density plot of an
amorphous foam prepared according to Example 1 to the specific stiffness vs. density plots of
the Inoue and Dunand foams and to the specific strength vs. density plot of trabecular (or
cancellous) bone;

- 1 [0018] FIG. 7B is a graph comparing the specific strength vs. density plot of an amorphous foam prepared according to Example 1 to the specific strength vs. density plots of the Inoue and Dunand foams and to the specific strength vs. density plot of trabecular (or cancellous) bone;
- 5 [0019] FIGs. 8A and 8C are scanning electron microscope (SEM) photographs at different magnifications of the cellular morphology of natural bone;
- [0020] FIGs. 8B and 8D are optical microscopy photographs at different magnifications of the cellular morphology of an amorphous metal foam according to one embodiment of the present invention;
- 10 [0021] FIG. 9 is a graph of the compressive loading responses of AMFs produced according to Example 1 having densities of 1.66 g/cc (83% porosity) and 0.76 g/cc (92% porosity);
- [0022] FIG. 10 is a graph comparing the density-dependent stiffness of the AMF produced according to Example 1 to the density-dependent stiffness of trabecular bone, the density-dependent stiffness of the Inoue AMFs and the density-dependent stiffness of the Dunand AMF; and
- 15 [0023] FIG. 11 is a graph comparing the density-dependent strength of the AMFs produced according to Example 1 to the density-dependent strength of trabecular bone, the density-dependent strength of the Inoue AMFs and the density-dependent strength of the Dunand AMFs.
- 20

DETAILED DESCRIPTION OF THE INVENTION

- [0024] The present invention is directed to amorphous metal foams (AMFs) capable of matching the mechanical properties of bone. Over the last decade, interest has increased in metallic porous scaffold substitutes for bone tissue engineering applications. For bone replacements, porosity is desired for promoting bone ingrowth and attachment, reducing the overall implant density to match that of adjacent bone, and enhancing plastic deformability to replicate the deformation behavior of bone. Furthermore, successful scaffold materials should provide mechanical support in order to preserve tissue volume and ultimately to facilitate tissue regeneration. An optimal scaffold should therefore exhibit mechanical performance that closely resembles that of natural bone in order to replicate its load-bearing capabilities. The most essential mechanical properties to be matched by the scaffold are bone loading stiffness and strength.
- 25
- 30
- [0025] When the scaffold's stiffness exceeds that of natural bone, stress concentration in the surrounding bone can cause bone failure. When the scaffold's stiffness is less than that of natural bone, stress concentration in the scaffold can cause implant failure as well as bone atrophy. This effect of stiffness mismatch, which gives rise to uneven load sharing between bone and implant, is known as stress shielding.
- 35

1 [0026] In addition to matching bone stiffness, the scaffold should also match or exceed the strength of natural bone. An equal or excess strength ensures that the implant has equivalent or better load bearing capabilities than natural bone.

5 [0027] Amorphous metals exhibit high strength and low stiffness compared to conventional crystalline metals. As such, amorphous metal foams (AMFs) may be suitable bone scaffold materials. For this purpose, two methods of producing structurally practical AMFs have been proposed. The first method synthesizes AMFs by precipitation of hydrogen dissolved in the liquid state (the "Inoue method"). The second method synthesizes AMFs by infiltration of salt performs and subsequent leaching of the salt (the "Dunand method").

10 [0028] Mechanical data has been reported for AMFs produced by the Inoue and Dunand methods. AMFs produced by the first method have density-dependent stiffnesses and strengths that are outside the respective ranges for bone. AMFs produced by the second method have density-dependent strengths that are inside the range for bone, but density-dependent stiffnesses that are outside the range for bone. Accordingly, neither the first nor the second methods have yet produced AMFs that would be desirable as bone replacements.

15 [0029] According to one embodiment of the present invention, AMFs exhibit both density-dependent strengths and stiffnesses that fall inside the respective ranges for bone. In particular, the AMFs exhibit density-dependent strengths and stiffnesses that closely match those properties in trabecular and/or cancellous bone. In one embodiment, for example, an AMF exhibits a density-dependent stiffness that closely matches that of bone, and exhibits a density-dependent strength that is equal to or greater than that of bone. In one exemplary embodiment, the AMF exhibits exhibit a density-dependent stiffness ranging from about $E = 640\rho^{3.75}$ to about $E = 2900\rho^{0.78}$, where $\rho < 1.7$ g/cc. The AMF may also exhibit a density-dependent strength greater than about $\sigma_y = 8.1\rho^{2.57}$, where $\rho < 1.7$ g/cc. In the power-law relations given by $E = 640\rho^{3.75}$, $E = 2900\rho^{0.78}$, and $\sigma_y = 8.1\rho^{2.57}$, E denotes the foam compressive loading stiffness (Young's Modulus) in MPa, σ_y denotes the foam strength (failure stress) in MPa, and ρ denotes the foam density in g/cc. Accordingly, in one embodiment of the present invention, an AMF has a density of less than about 1.7 g/cc, a compressive loading stiffness ranging from about $640\rho^{3.75}$ to about $2900\rho^{0.78}$, and a strength of greater than about $8.1\rho^{2.57}$.

20 [0030] In another embodiment of the present invention, the AMFs have specific stiffnesses substantially matching those of natural bone. In particular, the AMFs substantially match these properties in trabecular and/or cancellous bone. In one exemplary embodiment, an AMF has a density-dependent specific stiffness ranging from about $E_s = 620\rho^{2.81}$ to about $E_s = 2600$, where $\rho < 1.7$ g/cc. The upper limit of $E_s = 2600$ appears to be independent of density. In the power-law relation given by $E_s = 620\rho^{2.81}$ to about $E_s = 2600$, E_s denotes the foam specific loading stiffness (i.e. Young's Modulus divided by density) in J/g, and ρ denotes the foam density in g/cc.

1 [0031] According to yet another embodiment, the AMFs have specific strengths
substantially equal to or greater than those of natural bone, and of trabecular or cancellous
bone in particular. In one exemplary embodiment, an AMF has a density-dependent specific
strength equal to or greater than about $\rho_s = 5.16\rho^{2.37}$, where $\rho < 1.7$ g/cc. In the power-law
5 relation given by $\sigma_s = 5.16\rho^{2.37}$, σ_s denotes the foam specific strength (i.e. compressive
strength divided by density) in J/g, and ρ denotes the foam density in g/cc.

[0032] The base solids of the AMFs according to embodiments of the present invention
may be any metallic alloy composition that can form a vitrified amorphous state in bulk
dimensions (i.e., greater than 1mm), and that would result in the density-dependent foam
10 strength and stiffness discussed above. Non-limiting examples of suitable alloy compositions
include Zr-based alloys, Ti-based alloys, Al-based alloys, Ni-based alloys, Fe-based alloys,
La-based alloys, Cu-based alloys, Ce-based alloys, Mg-based alloys, Au-based alloys, Pt-
based alloys, and Pd-based alloys. One exemplary embodiment of a suitable alloy
composition is Pd₄₃Ni₁₀Cu₂₇P₂₀.

15 [0033] The AMFs according to the present invention may be prepared by any suitable
method so long as the resulting AMF exhibits the density-dependent strengths and stiffnesses
discussed above. In general, AMFs may be prepared by one of the following methods: 1)
expansion of powder compacts involving powder mixtures of the amorphous metal and a
blowing agent; 2) precipitation of hydrogen dissolved in the liquid state; 3) infiltration of salt
20 performs and subsequent leaching of salt; and 4) *in situ* decomposition of a metal hydride.
However, these methods have not yet been able to produce an AMF having the desired
density-dependent properties discussed above.

[0034] According to one exemplary embodiment of the present invention, an AMF
having the desired density-dependent strength and stiffness properties is prepared by a new
25 method involving the expansion of bubbles entrained in liquid or supercooled liquid. First, a
two-phase mixture of a suitable alloy in its liquid state and a chemically non-reacting
propellant gas is prepared. The mixture is placed in an inert gas atmosphere under a pressure,
 p_i . The mixture is held a temperature T_i that is greater than the optimum temperature for
foaming, T_o . The mixture is then brought to the optimum temperature T_o , and foam
30 expansion is induced by dropping the pressure to the optimum pressure, p_o , where $p_o < p_i$.
The two-phase mixture is then quenched to a temperature below the glass transition
temperature of the alloy, thereby producing an amorphous metal foam.

[0035] In preparing AMFs according to this method, the parameters used may vary
depending on the alloy used. In one embodiment, T_i is any temperature above the glass
35 transition temperature of the alloy, but above the melting point of the alloy. For example, for
a Pd₄₃Ni₁₀Cu₂₇P₂₀ alloy, T_i may be about 900°C. In another embodiment, T_o may be any
temperature above the glass transition temperature of the alloy, but between the nose of the
time-temperature-transformation (TTT) curve and the melting point. For example, for a

1 Pd₄₃Ni₁₀Cu₂₇P₂₀ alloy, T_o may be about 420°C. According to yet another embodiment, p_i
may be the highest pressure allowed by the container holding the mixture at hydrostatic
strength. For example, for a Pd₄₃Ni₁₀Cu₂₇P₂₀ alloy, p_i may be about 1 bar. In still another
embodiment, p_o may be the lowest pressure attainable by mechanical evacuation. For
5 example, for a Pd₄₃Ni₁₀Cu₂₇P₂₀ alloy, p_o may be about 0.01 mbar.

[0036] The two-phase mixture used in the method may be generated by any suitable
method of gas entrainment in a liquid. Nonlimiting examples of suitable such methods
include mechanical entrapment, gas dissolution, and the use of gas releasing agents.

[0037] The chemically non-reacting propellant gas used in the alloy mixture may be any
10 gas composition that can be entrained in the liquid but that does not react with it to
substantially degrade its vitrifying ability or viscoplastic forming ability. Nonlimiting
examples of suitable such gases include helium, argon, air, nitrogen, hydrogen, water vapor,
carbon monoxide and carbon dioxide. When gas releasing agents are used, any gas releasing
agent composition may be used that decomposes to release a gas that can be entrained in the
15 liquid without chemically reacting with it to substantially degrade its vitrifying ability or
viscoplastic forming ability. Nonlimiting examples of suitable such gas releasing agents
include water vapor-releasing agents, hydrogen-releasing agents, carbon monoxide-releasing
agents, carbon dioxide-releasing agents, and nitrogen-releasing agents.

[0038] This foam synthesis route utilizes a ductile yet viscous state of the undercooled
20 liquid to develop amorphous metallic foams by expansion of entrained gas bubbles. Liquid
ductility is desired to enable plastic elongation of membranes, while high liquid viscosity is
required to inhibit bubble sedimentation during foaming. For undercooled liquids, ductility
increases by increasing temperature while viscosity increases by decreasing temperature.
Therefore, the optimum temperature for foaming, T_o , is that at which the liquid exhibits
25 adequate ductility as well as adequately high viscosity. However, liquid stability against
crystallization minimizes at intermediate temperatures in undercooled liquid regions, limiting
the available time for processing at those temperatures. Therefore, the foaming time at T_o is
stringently constrained by rate of crystallization kinetics.

[0039] One example of an AMF produced by this method is described below in Example
30 1. In Example 1, Pd₄₃Ni₁₀Cu₂₇P₂₀ is used to prepare the AMF. As shown in the time-
temperature-transformation (TTT) diagram in FIG. 1A, the Pd₄₃Ni₁₀Cu₂₇P₂₀ alloy has a 200
second time window at 420°C which can be utilized for foaming. The temperature dependent
viscosity of Pd₄₃Ni₁₀Cu₂₇P₂₀ liquid is shown in FIG. 1B. By extrapolation, the liquid
viscosity at 420°C is about 1×10^4 Pa-s, which is adequately high to inhibit micro-bubble
35 floatation. FIG. 1C depicts the limits of strain rate sensitivity of Pd₄₃Ni₁₀Cu₂₇P₂₀ liquid.
Within these strain rate limits, flow can be maintained Newtonian giving rise to ideal liquid
ductility. By extrapolation, the strain rate limit at 420°C is about 1 s^{-1} , which confines a range

1 of liquid ductility that is adequately broad for foaming. Therefore, T_o for Pd₄₃Ni₁₀Cu₂₇P₂₀ is 420°C.

[0040] Example 1 below illustrates one exemplary method of making an AMF from a Pd₄₃Ni₁₀Cu₂₇P₂₀ liquid. The following Examples are provided for illustrative purposes only
5 and are not intended to limit the scope of the present invention.

Example 1

[0041] A Pd₄₃Ni₁₀Cu₂₇P₂₀ alloy ingot together with H₃BO₃ powder was enclosed in a quartz tube under 1-bar pressure of argon, and heated to 900°C for approximately 3-5 minutes to facilitate gas release and entrainment in the liquid. The tube containing the mixture was
10 then immersed in molten tin at 420°C, and allowed to stand for approximately 30-60 seconds to attain thermal equilibration. Then, pressure was reduced to below 0.01 mbar. Finally, the mixture was rapidly quenched in water.

[0042] FIG. 2 is a photograph of the AMF produced according to Example 1. The AMF had a density of 1.16 g/cc (88% porosity). FIG. 2 also depicts a pore-free button of
15 equivalent mass, which is shown to demonstrate the nearly 10-fold increase in volume produced by foaming. FIG. 3 is an x-ray diffractogram verifying the amorphous nature of the AMF produced according to Example 1. FIG. 4 depicts two other foams prepared according to Example 1, but having densities of 0.93 g/cc (90% porosity). As shown in FIG. 3, these foams float in water. The porosities of the foams produced according to Example 1 were
20 assessed using the Archimedes method as well as the graphical method.

[0043] FIG. 5 depicts a graph comparing the compressive loading responses of the AMF prepared according to Example 1 and trabecular bone. As evidenced by the stress-strain plots, the AMF prepared according to Example 1 closely matches the compressive loading response of bone.

[0044] In addition, in FIG. 6, the compressive strengths of the AMF prepared according to Example 1 and trabecular bone are plotted against their respective elastic moduli. The slopes of the compressive strength-elastic modulus plots constitute the elastic strain limits. As shown in FIG. 6, the slopes of the AMF prepared according to Example 1 and trabecular
25 bone are comparable. Therefore, the AMF prepared according to Example 1 has elastic stability similar to bone.

[0045] The AMFs prepared according to Example 1 were compared with the reported data on AMFs prepared by precipitation of hydrogen dissolved in the liquid state (hereafter the "Inoue AMFs"). This method is described in detail in T. Wada, and A. Inoue, "Formation of Porous Pd-based Bulk Glassy Alloys by a High Hydrogen Pressure Melting-Water
35 Quenching Method and Their Mechanical Properties," Mater. Trans. 46, 2777 (2005) and T. Wada, K. Takenaka, N. Nishiyama, and A. Inoue, "Formation and Mechanical Properties of Porous Pd-Pt-Cu-P Bulk Glassy Alloys," Mater. Trans. 46, 2777 (2005), the entire contents of which are incorporated herein by reference.

1 [0046] The AMFs prepared according to Example 1 were also compared with the
reported data on AMFs prepared by infiltration of salt performs and subsequent leaching of
salt (hereafter the "Dunand AMFs"). This method is described in detail in H. Brothers, and
D. C. Dunand, "Ductile Bulk Metallic Glass Foams," *Adv. Mater.* **17**, 484 (2005), H.
5 Brothers, and D. C. Dunand, "Plasticity and Damage of Cellular Amorphous Metals," *Acta*
Mater. **53**, 4424 (2005), and H. Brothers, and D. C. Dunand, "Amorphous Metal Foams,"
Scripta Mater. **54**, 513 (2006), the entire contents of which are incorporated herein by
reference.

10 [0047] FIG. 7A depicts a graph comparing the specific stiffnesses plotted against density
of the AMF prepared according to Example 1 to the specific stiffnesses plotted against
density of the Inoue and Dunand AMFs and the specific stiffnesses plotted against density of
trabecular (or cancellous) bone. As shown in FIG. 7A, the AMF prepared according to
Example 1 exhibits specific stiffnesses substantially matching those of bone. As also shown
15 the upper limit of the specific stiffness appears to be independent of density (shown by the
horizontal line in the drawing). In addition, as can be seen from FIG. 7A, the AMF prepared
according to Example 1 matches the specific stiffness properties of bone much better than do
the Inoue and Dunand AMFs.

20 [0048] FIG. 7B depicts a graph comparing the specific strengths plotted against density
of the AMF prepared according to Example 1 to the specific strengths plotted against density
of the Inoue and Dunand AMFs and the specific strengths plotted against density of
trabecular (or cancellous) bone. As shown in FIG. 7B, the AMF prepared according to
Example 1 exhibits specific strengths substantially matching those of bone. As also shown in
FIG. 7B, the AMF prepared according to Example 1 matches the specific strength properties
of bone much better than do the Inoue and Dunand AMFs.

25 [0049] FIGs. 8A and 8C are scanning electron microscope (SEM) photographs of the
cellular morphology of natural bone, and FIGs. 8B and 8C are optical microscopy
photographs of the cellular morphology of the AMF prepared according to Example 1. A
comparison of the photographs in FIGs. 8A through 8D shows that the AMF produced
according to Example 1 has a cellular morphology similar to that of natural bone. In the
30 method of making an AMF outlined in Example 1, cell volume fraction and size distribution
can be tailored by the foam processing parameters. As such, the closed cell architecture of
the AMF is suitable for promoting cell attachment and migration.

Experimental Example 1

[0050] AMFs were prepared having densities ranging from 0.76 to 1.66 g/cc.

35 Compressive testing of each AMF was performed. Cylindrical specimens with polished and
parallel loading surfaces having diameters of 18 mm and heights ranging between 25 and 30
mm were prepared for mechanical testing. A servo-hydraulic Materials Testing System with
a 50-kN load cell was utilized for the loading tests. Strain rates of $1 \times 10^{-4} \text{ s}^{-1}$ were applied.

1 Strains were measured using a linear variable displacement transducer (LVDT). The
compressive loading responses of the 1.66g/cc (83% porosity) and 0.76g/cc (92% porosity)
AMFs are shown in FIG. 9. The loading stiffness is taken to be the slope of the linear
loading response prior to failure, while the strength is taken to be the peak stress at failure.
5 [0051] FIG. 10 depicts a plot of density-dependent stiffness against that of bone. In FIG. 10,
exemplary inventive AMFs having density-dependent stiffnesses ranging from $E = 640\rho^{3.75}$
to about $E = 2900\rho^{0.78}$ (where $\rho < 1.7$ g/cc) are compared to natural bone and to the Inoue
AMFs and Dunand AMFs. The dotted lines represent the upper and lower bounds of density-
dependent stiffnesses according to the formulae $E = 640\rho^{3.75}$ and $E = 2900\rho^{0.78}$ (where $\rho <$
10 1.7 g/cc). As shown in FIG. 10, the AMFs prepared according to Example 1 have density-
dependent stiffnesses closely matching that of bone, but the Inoue AMFs and Dunand AMFs
have density-dependent stiffnesses outside the range needed to match the density-dependent
stiffness of bone.

[0052] FIG. 11 is a plot of density-dependent strength against that of bone. In FIG. 11,
15 exemplary inventive AMFs having density-dependent strengths bounded above $\sigma_y = 8.1\rho^{2.57}$
(where $\rho < 1.7$ g/cc) are compared to natural bone and to the Inoue AMFs and Dunand
AMFs. The dotted line represents the lower bound of density-dependent strength according
to the formula $\sigma_y = 8.1\rho^{2.57}$ (where $\rho < 1.7$ g/cc). As shown in FIG. 11, the AMFs prepared
according to Example 1 have density-dependent strengths closely matching those of bone.
20 Accordingly, the AMF prepared according to Example 1 exhibits static load-bearing
capabilities closely matching those of bone. As also shown in FIG. 11, while the Dunand
AMFs have density-dependent strengths similar to that of bone, the Inoue AMFs do not.
Even though the Dunand AMFs have density-dependent strengths similar to that of bone,
these AMFs do not have density-dependent stiffnesses similar to that of bone (as shown in
25 FIG. 6), and are thus rendered undesirable as bone replacements.

[0053] While the present invention has been illustrated and described with reference to
certain exemplary embodiments, those of ordinary skill in the art understand that various
modifications and changes may be made to the described embodiments without departing
from the spirit and scope of the present invention as defined by the following claims.
30

35

1 WHAT IS CLAIMED IS:

1. An amorphous metal foam comprising a density-dependent stiffness substantially matching a density-dependent stiffness of natural bone and a density-dependent strength substantially equal to or greater than a density-dependent strength of natural bone.

5

2. The amorphous metal foam according to claim 1, further comprising a density-dependent sound velocity substantially matching a density-dependent sound velocity of natural bone.

10

3. The amorphous metal foam according to claim 1, wherein the amorphous metal foam comprises a density-dependent stiffness ranging from about $640\rho^{3.75}$ to about $2900\rho^{0.78}$, and a density dependent strength greater than about $8.1\rho^{2.57}$, wherein ρ is less than about 1.7 g/cc.

15

4. The amorphous metal foam according to claim 1, wherein the amorphous metal foam comprises an amorphous alloy selected from the group consisting of Zr-based alloys, Ti-based alloys, Al-based alloys, Fe-based alloys, La-based alloys, Cu-based alloys, Ce-based alloys, Mg-based alloys, Au-based alloys, Pt-based alloys and Pd-based alloys.

20

5. The amorphous metal foam according to claim 1, wherein the amorphous metal foam comprises an amorphous Pd-based alloy.

6. The amorphous metal foam according to claim 5, wherein the amorphous Pd-based alloy is $\text{Pd}_{43}\text{Ni}_{10}\text{Cu}_{27}\text{P}_{20}$.

25

7. An amorphous metal foam comprising a density-dependent stiffness ranging from about $640\rho^{3.75}$ to about $2900\rho^{0.78}$, and a density dependent strength greater than about $8.1\rho^{2.57}$, wherein ρ is less than about 1.7 g/cc.

30

8. The amorphous metal foam according to claim 7, wherein the amorphous metal foam comprises an amorphous alloy selected from the group consisting of Zr-based alloys, Ti-based alloys, Al-based alloys, Fe-based alloys, La-based alloys, Cu-based alloys, Ce-based alloys, Mg-based alloys, Au-based alloys, Pt-based alloys and Pd-based alloys.

35

9. The amorphous metal foam according to claim 7, wherein the amorphous metal foam comprises an amorphous Pd-based alloy.

- 1 10. The amorphous metal foam according to claim 9, wherein the amorphous Pd-
based alloy is Pd₄₃Ni₁₀Cu₂₇P₂₀.
- 5 11. The amorphous metal foam according to claim 7, further comprising a density-
dependent specific stiffness ranging from about $620\rho^{2.81}$ to about 2600, wherein $\rho < 1.7$ g/cc.
12. The amorphous metal foam according to claim 7, further comprising a density-
dependent specific strength equal to or greater than about $5.16\rho^{2.37}$, wherein $\rho < 1.7$ g/cc.
- 10 13. A method of making an amorphous metal foam, the method comprising:
 mixing a metal alloy liquid with a chemical non-reacting propellant gas;
 sealing the mixture in a container in an inert gas atmosphere at an initial
 pressure determined by the hydrostatic pressure of the container;
 holding the mixture at an initial temperature above a glass transition
15 temperature of the metal alloy and above a melting point of the metal alloy;
 reducing the temperature of the mixture to an optimum temperature above the
 glass transition temperature of the metal alloy and below the melting point of the metal alloy;
 reducing the initial pressure to an optimum pressure below the initial pressure;
 and
20 quenching the mixture to a final temperature below the glass transition
 temperature of the metal alloy to produce an amorphous metal foam.
14. The method according to claim 13, wherein the propellant gas is selected from
 the group consisting of helium, argon, air, nitrogen, hydrogen, water vapor, carbon monoxide
25 and carbon dioxide.
15. The method according to claim 13, wherein the metal alloy is selected from
 the group consisting of Zr-based alloys, Ti-based alloys, Al-based alloys, Fe-based alloys,
 La-based alloys, Cu-based alloys, Ce-based alloys, Mg-based alloys, Au-based alloys, Pt-
30 based alloys and Pd-based alloys.
16. The method according to claim 13, wherein the metal alloy is a Pd-based
 alloy.
- 35 17. The method according to claim 16, wherein the Pd-based alloy is
 Pd₄₃Ni₁₀Cu₂₇P₂₀.

1 18. The method according to claim 13, wherein the amorphous metal foam
comprises a density-dependent stiffness substantially matching a density-dependent stiffness
of natural bone and a density-dependent strength substantially equal to or greater than a
density-dependent strength of natural bone.

5 19. The method according to claim 13, wherein the amorphous metal foam
comprises a density-dependent sound velocity substantially matching a density-dependent
sound velocity of natural bone.

10 20. The method according to claim 13, wherein the amorphous metal foam
comprises a density-dependent stiffness ranging from about $640\rho^{3.75}$ to about $2900\rho^{0.78}$, and a
density dependent strength greater than about $8.1\rho^{2.57}$, wherein ρ is less than about 1.7 g/cc.

15

20

25

30

35

FIG. 1A

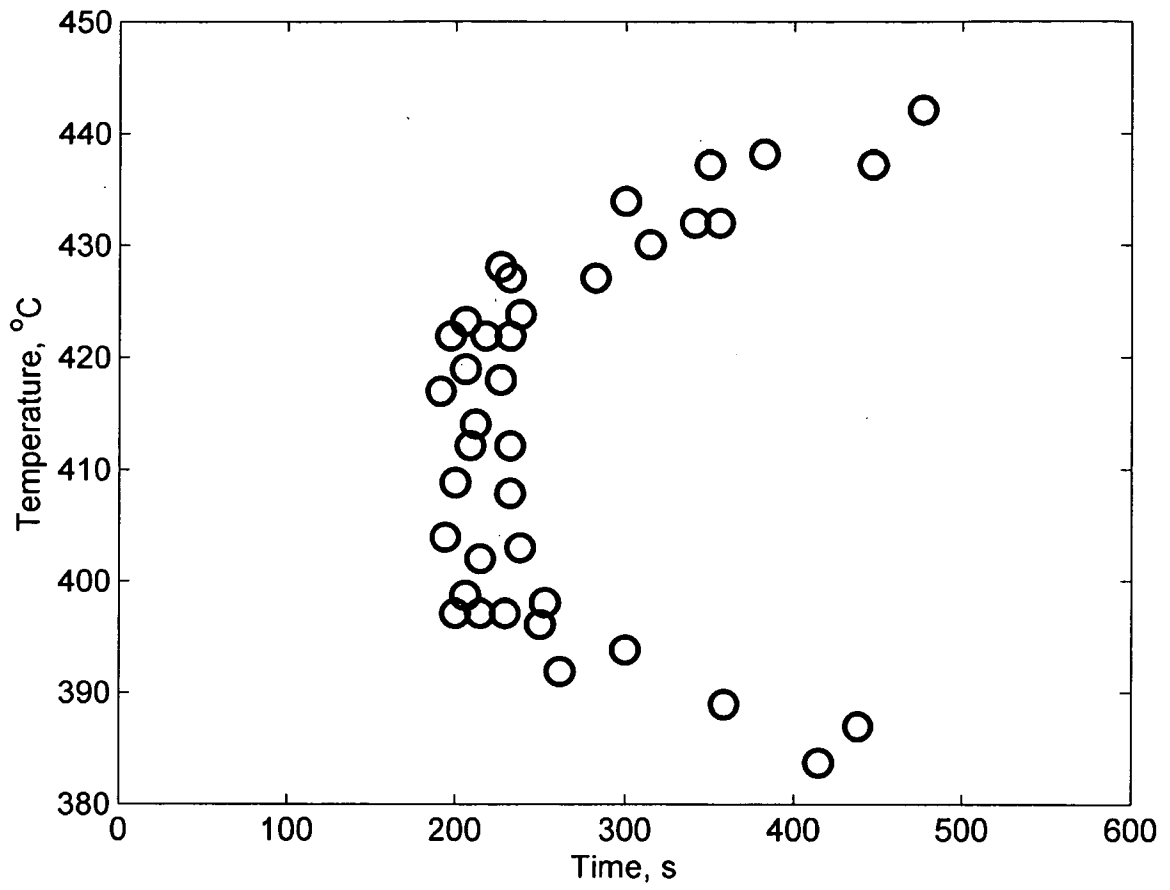


FIG. 1B

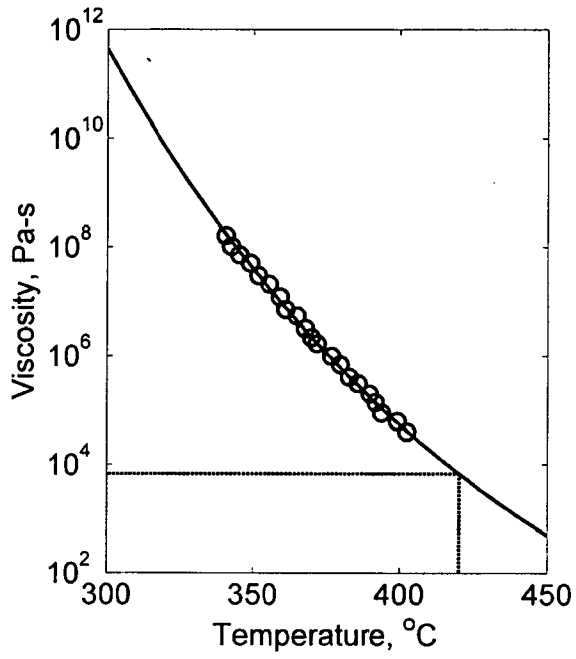


FIG. 1C

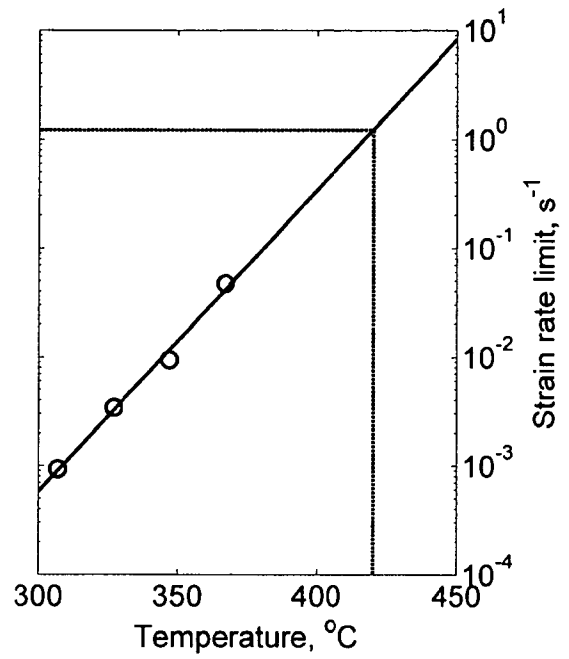


FIG. 2

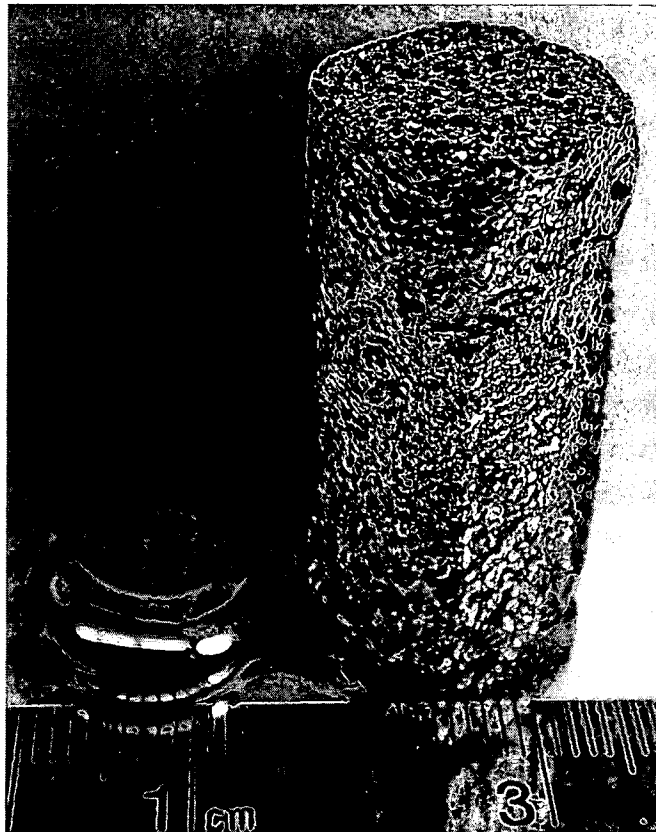


FIG. 3

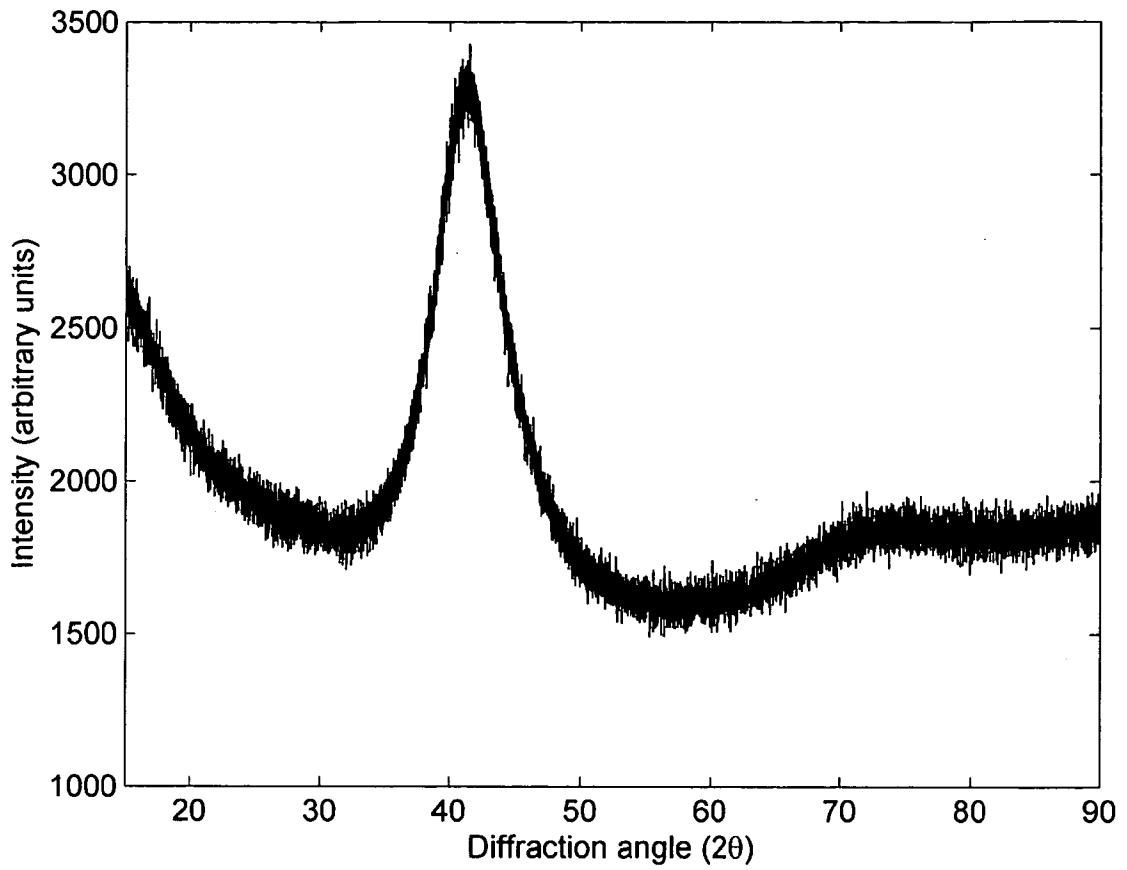


FIG. 4

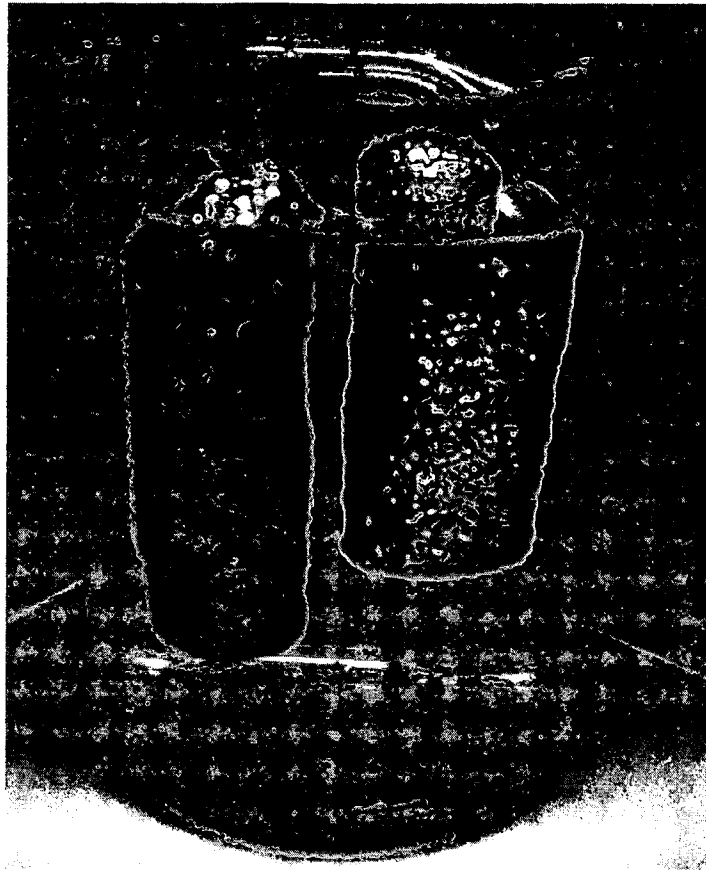


FIG. 9

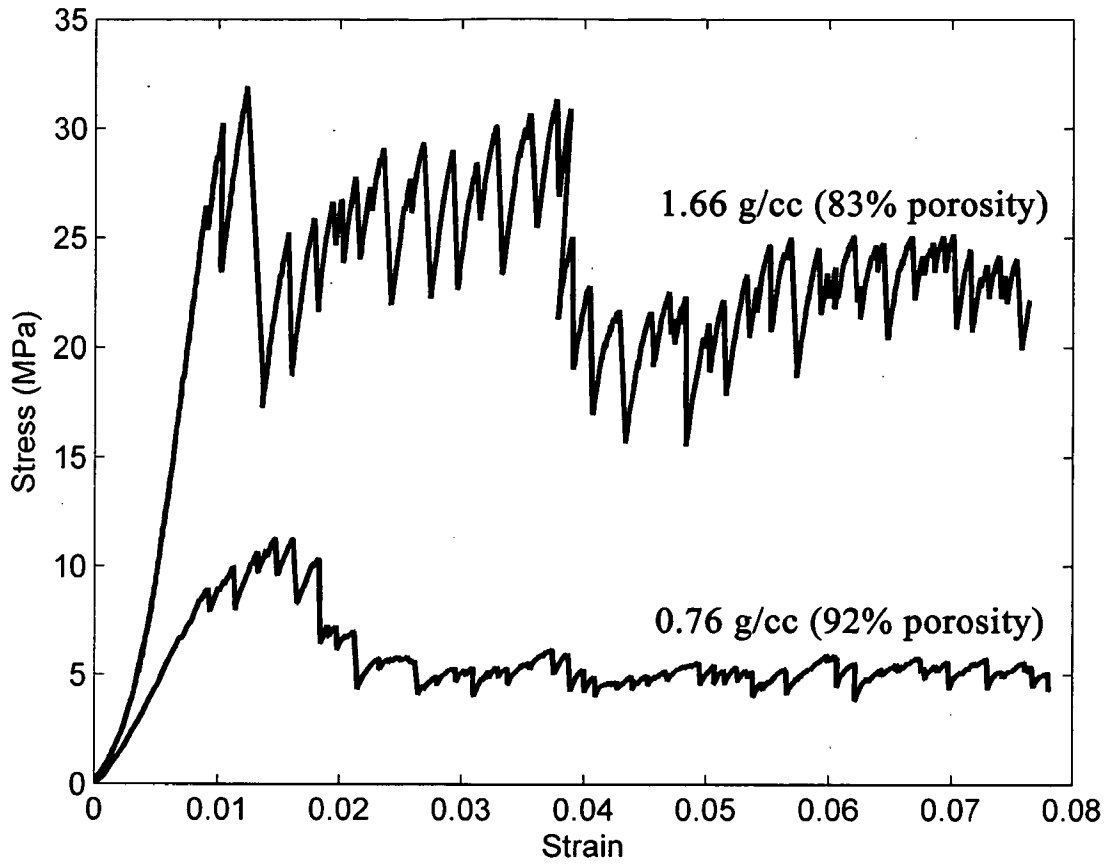


FIG. 10

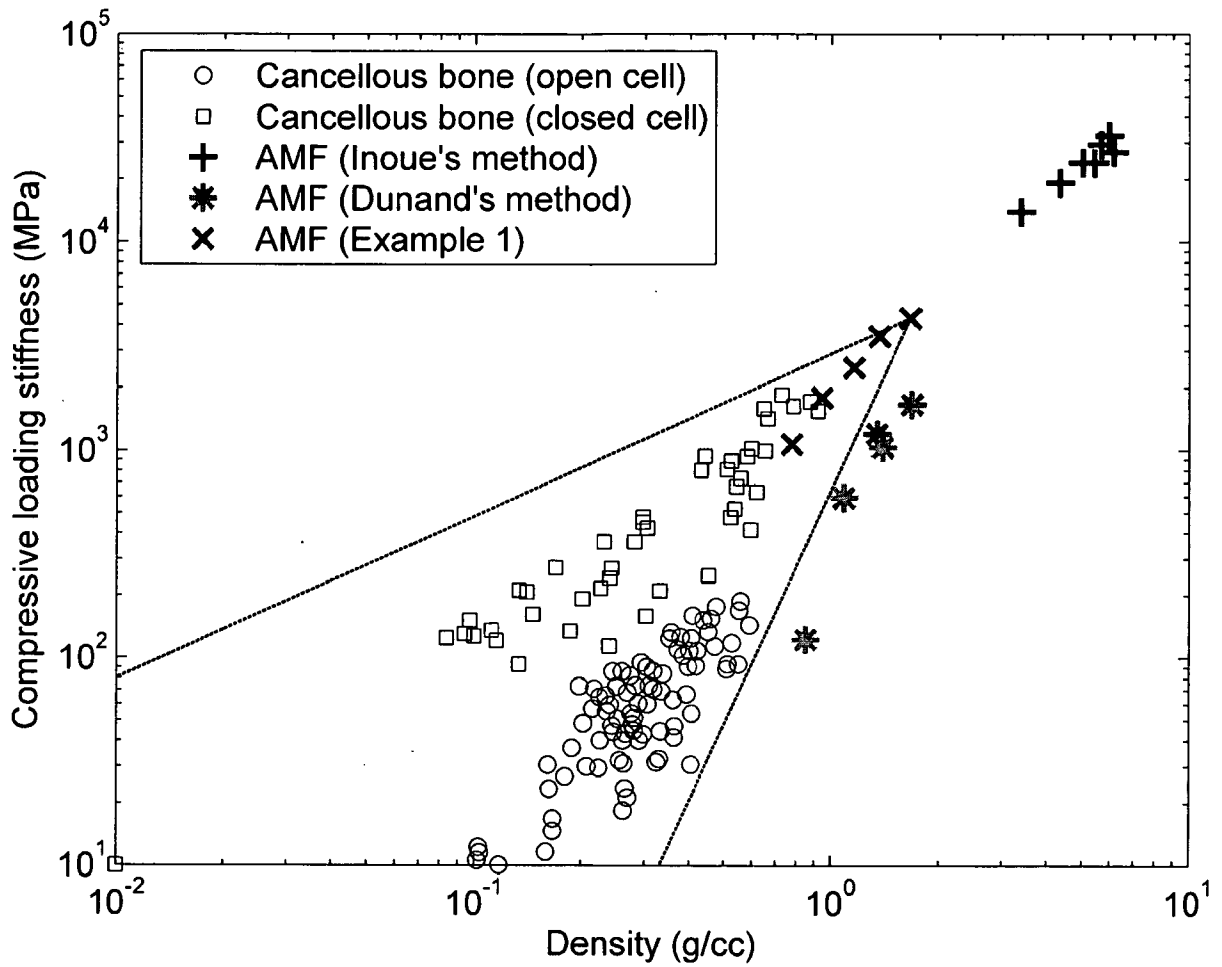


FIG. 11

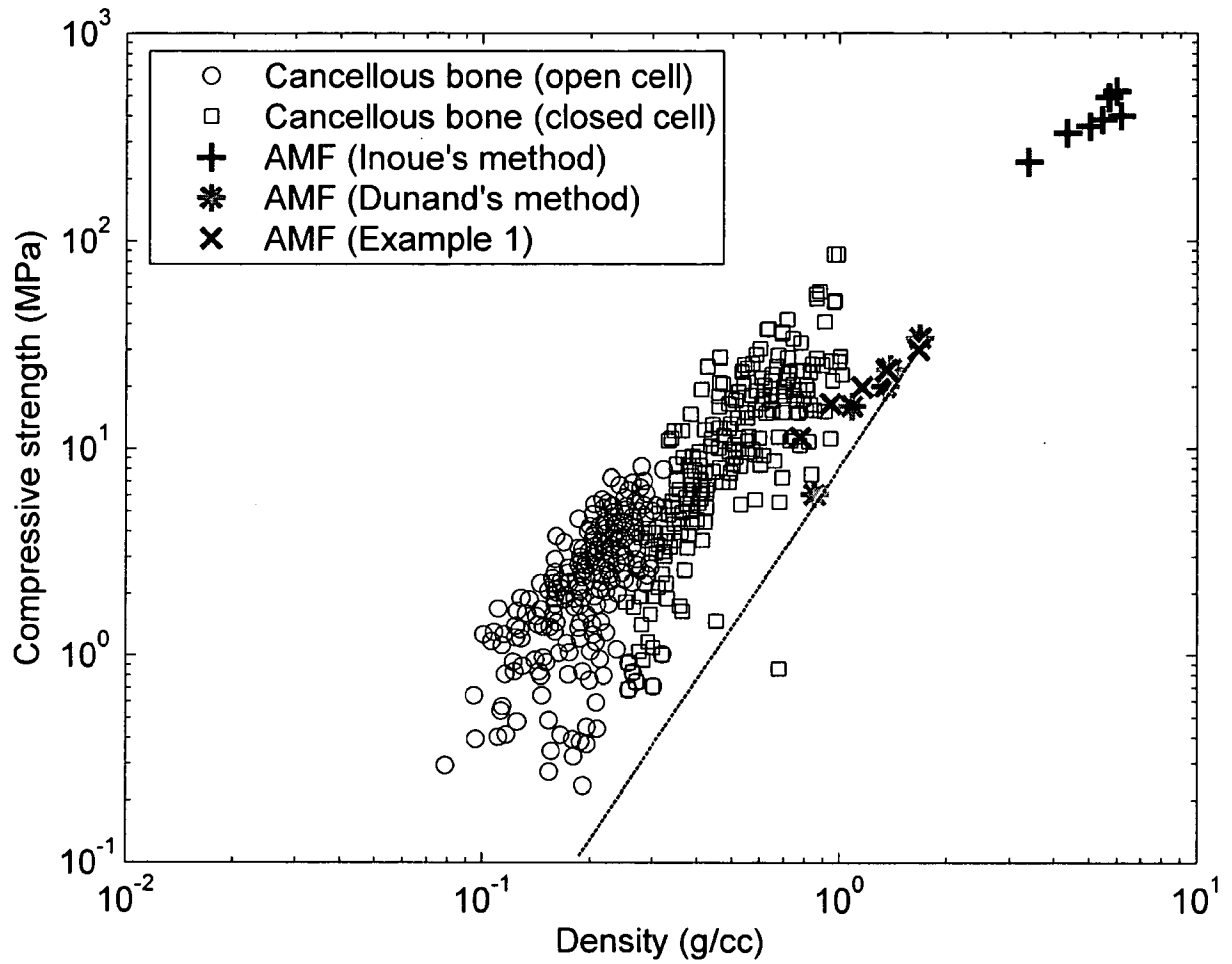


FIG. 8A

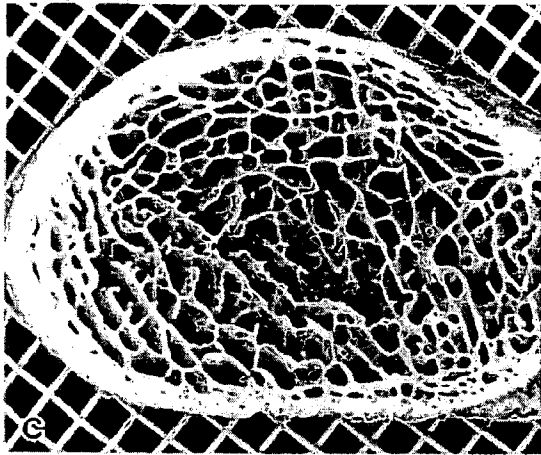


FIG. 8B

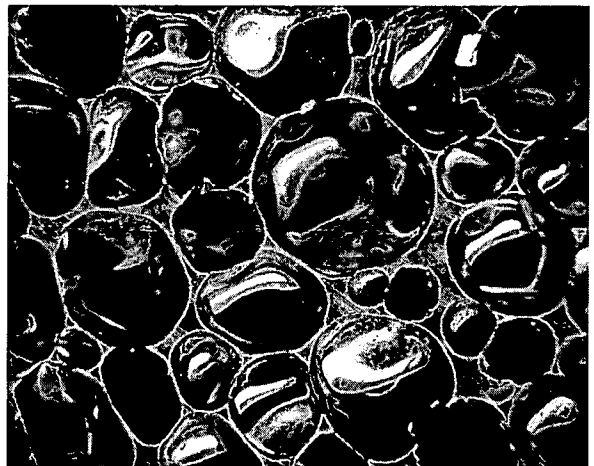
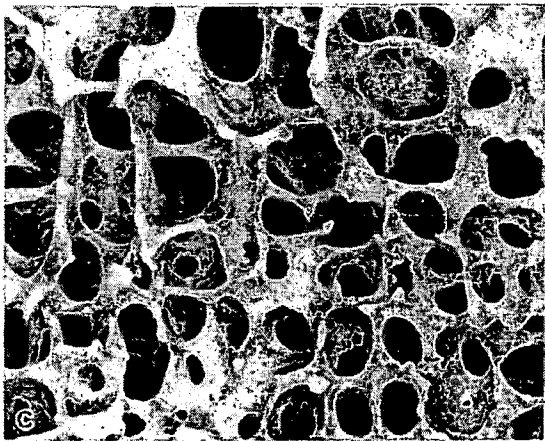
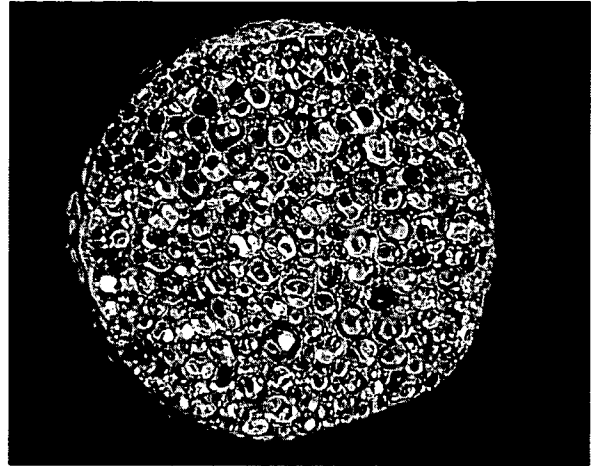


FIG. 8C

FIG. 8D

FIG. 5

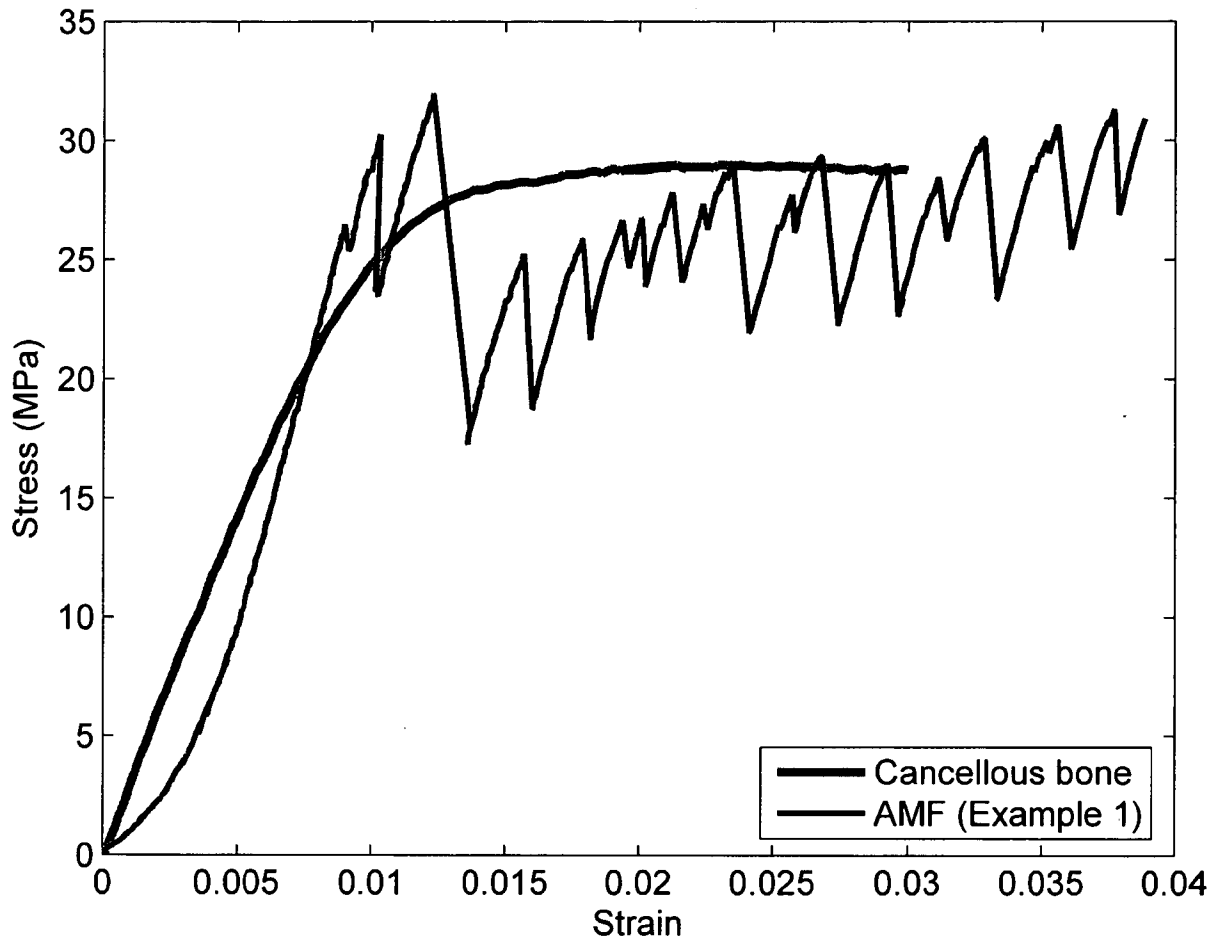


FIG. 6

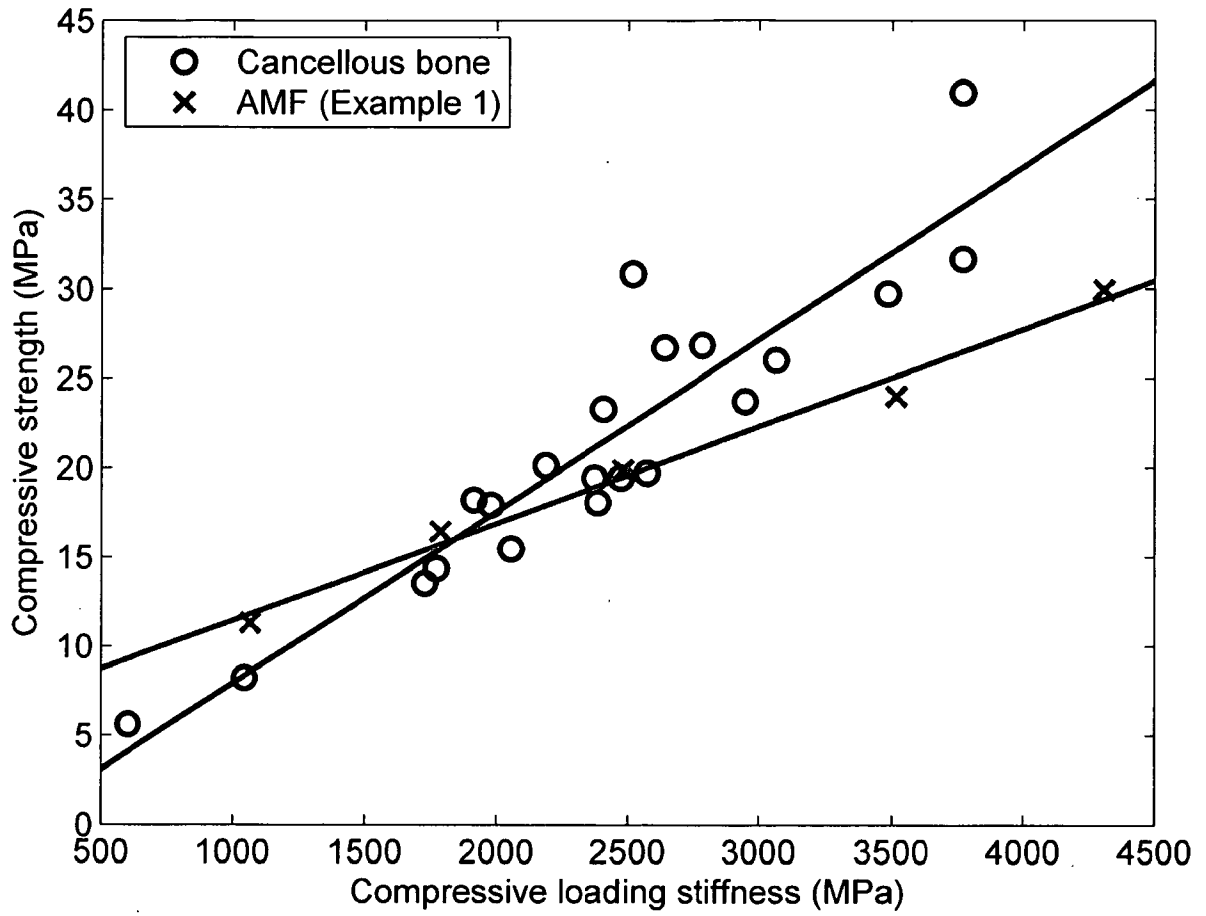


FIG. 7A

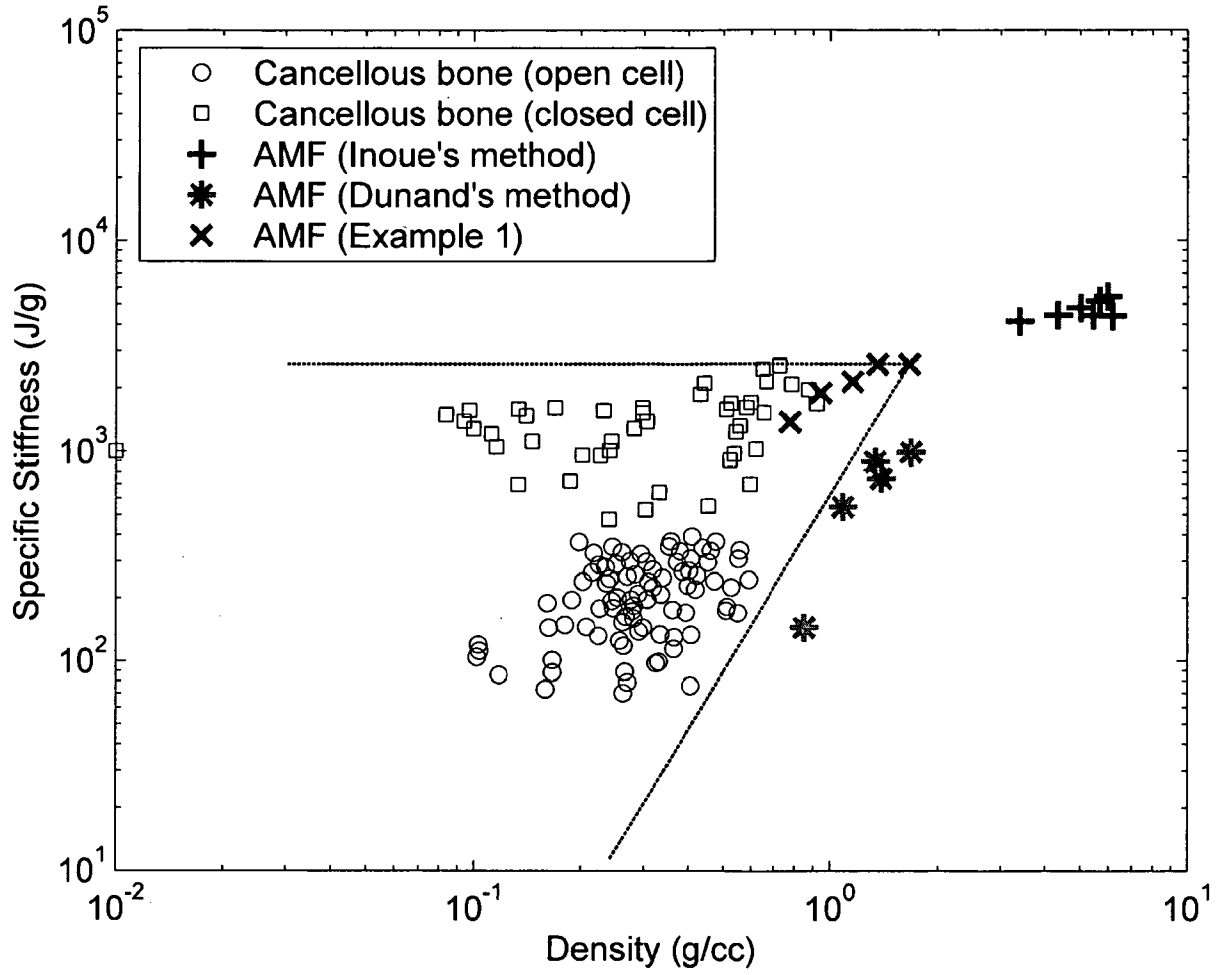


FIG. 7B

